Reliability-based multiobjective optimization using the satisficing trade-off method

Bulletin of the JSME

Vol.X, No.X, XXXX

Reliability-based multiobjective optimization using the satisficing trade-off method

Nozomu KOGISO*, Ryo KODAMA* and Masahiro TOYODA*

* Department of Aerospace Engineering, Osaka Prefecture University

1-1 Gakuen-Cho, Naka-Ku, Sakai, Osaka 599-8531, Japan

E-mail: kogiso@aero.osakafu-u.ac.jp

Received 15 August 2014

Abstract

This study proposes a reliability-based multiobjective optimization (RBMO) approach using the satisficing trade-off method (STOM). STOM is a multiobjective optimization method that obtains a highly accurate single Pareto solution, regardless of the shape of the Pareto set. By introducing an aspiration level, STOM transforms the multiobjective optimization problem into the equivalent single objective problem. When the given Pareto solution is not satisfactory, the search process is repeated with a different aspiration level, which is selected using the automatic trade-off method, for example. RBMO considers multiobjective optimization under reliability constraints that consider uncertainties in the design parameters. In this study, the reliability is evaluated by the first-order reliability method. Therefore, the optimization problem is formulated as a conventional double-loop approach. However, the validity of the proposed method can be illustrated without a decoupled reliability-based design approach. Through numerical examples, the proposed method is shown to obtain an accurate Pareto solution for the RBMO problem. In addition, compared to multiobjective particle swarm optimization, parametrically changing the aspiration level produces a more accurate, uniformly distributed, and diverse Pareto set. The tracking ability of Pareto solutions with the same aspiration level is investigated in terms of the target reliability, which clarifies that the shift in the dominant failure mode influences the kink in the tracking trajectory. Finally, an analysis of the automatic trade-off method demonstrates that the desired Pareto solution can be obtained by updating the aspiration level, even when the Pareto surface is nonlinear.

Key words : Reliability-Based Multiobjective Optimization, Satisficing Trade-Off Method, Pareto Set, Automatic Trade-Off Analysis, First-Order Reliability Method

1. Introduction

Design problems are essentially defined in terms of multiobjective optimization [Mittinen, 2004]. However, most design problems adopt a single objective optimization method, whereby one objective function is selected from the many performance indices, and the other objectives are transformed to equivalent constraint conditions. Recently, multiobjective optimization has become popular, and has been applied to a variety of engineering design problems. Various evolutionary methods have been developed, such as multiobjective genetic algorithms [Deb et al., 2002] and multiobjective particle swarm optimization (MOPSO) [Reyes-Sierra and Coello Coello, 2006].

Design parameters such as material properties and applied loads have a number of uncertainties. Their performance measures also include uncertainties, because these are defined as a function of the uncertain parameters. In reliability analyses [Madsen et al., 1986] that apply probabilistic theory, uncertain parameters are defined as probabilistic random variables, and structural failure (i.e., when some performance measure exceeds its allowable range) is evaluated probabilistically. The first-order reliability method (FORM) [Rackwitz and Fiessler, 1978] is one of the primary techniques for evaluating reliability. FORM first transforms the random variables to independent standardized normal distribution variables, and then the reliability index β is evaluated as the minimum distance between the limit state surface ($h(\boldsymbol{u}) = 0$) and the origin in the standardized normal distribution space ($\boldsymbol{U}$-space). The failure probability is approximated as $P_f = \Phi(-\beta)$,

where $\Phi()$ is the probability distribution function of the standardized normal distribution. Since FORM must evaluate the minimum distance, it is implemented as an iterative calculation using the Rackwitz–Fiessler method [Rackwitz and Fiessler, 1978] or nonlinear programming.

Reliability-based design optimization (RBDO) integrates a reliability analysis with an optimization method [Choi et al., 2007, Valdebenito and Schuëller, 2010]. For example, RBDO can be used to obtain the minimum-weight design under given reliability constraints, or the maximum-reliability design under given weight constraints. As the reliability analysis also requires iterative calculations, RBDO is formulated as a time-consuming double-loop approach. Some computationally efficient decoupled approaches have been proposed, such as the single-loop single-vector (SLSV) method [Chen et al., 1997] and sequential optimization and reliability assessment (SORA) [Du and Chen, 2004]. The development of these efficient methods has popularized RBDO, which has subsequently been applied to many engineering design problems.

In contrast, research on reliability-based multiobjective optimization (RBMO), which combines multiobjective optimization with reliability analysis, is at an earlier stage [Deb et al., 2009, Sinha,2007, Li et al., 2011, Rangavajhala and Mahadevan, 2011, Greiner and Hajela, 2012]. Most researches have focused on multiobjective genetic algorithms, particularly NSGA-II [Deb et al., 2002]. To improve the computational efficiency of the evolutionary approach, one of the present authors proposed a hybrid-type MOPSO for the RBMO problem [Kogiso et al., 2012, Kogiso and Kawaji, 2013]. This hybrid MOPSO incorporates a constraint satisfaction technique using gradient information. The technique has two functions: moving design candidates with constraint violations to the feasible region using sensitivity information from the violated constraints, and then moving these to the feasible boundary using the bisection method. The hybrid MOPSO successfully obtains the Pareto set with high accuracy in the early stages of the search. The computational efficiency of the method is superior to that of conventional evolutionary algorithms like NSGA-II. However, the computational efficiency is still inferior to that of mathematical programming methods.

This study proposes a new method by applying the satisficing trade-off method (STOM) [Nakayama and Sawaragi, 1984] to RBMO to efficiently obtain a Pareto solution of the RBMO problem. STOM has been applied to numerous engineering design problems, e.g., [Nakayama et al., 1995, Kitayama and Yamazaki, 2012], but has not yet been applied to the RBMO problem. STOM is a multiobjective optimization method that obtains a single, highly accurate Pareto solution, regardless of the shape of the Pareto set. By introducing an aspiration level that corresponds to the user's preference for each objective function, STOM transforms the multiobjective optimization problem into the equivalent single objective problem. Mathematical programming techniques can be applied to the transformed problem, meaning that STOM obtains a Pareto solution efficiently. In addition, a highly diverse and uniformly distributed Pareto set can be obtained by parametrically changing the aspiration level. STOM is an interactive approach, because the search process is repeated by changing the aspiration level until the user is satisfied with the solution. The automatic trade-off analysis method [Nakayama, 1992] is one way of updating the aspiration level using sensitivity information.

Note that the efficient single-loop algorithm for RBMO is not adopted in this study. As STOM produces the equivalent single objective optimization problem, it is possible to adopt efficient RBDO methods such as SLSV or SORA. However, this study adopts the FORM reliability analysis and performs a double-loop optimization, because our aim is to investigate STOM applied to RBMO. Efficient decoupled RBDO methods will be applied at a later date to improve the computational efficiency.

Through numerical examples, the efficiency of STOM for the RBMO problem is discussed by comparing its performance with that of the hybrid-type MOPSO [Kogiso et al., 2012, Kogiso and Kawaji, 2013]. It is shown that the proposed method obtains a more accurate, uniformly distributed, and diverse Pareto set than that of MOPSO, and that the Pareto front can be obtained by changing the aspiration level parametrically. The tracking ability of Pareto solutions with the same aspiration level is investigated in terms of the target reliability, and we find that the shift in dominant failure mode influences the kink of the tracking trajectory. Finally, the automatic trade-off analysis shows that the desired Pareto solution can be obtained by updating the aspiration level, even when the Pareto surface is nonlinear.

2. Reliability-Based Multiobjective Optimization

RBMO considers the reliability constraints imposed by uncertainties in design parameters such as material properties and applied loads. In this study, design variables and random variables are denoted as $\boldsymbol{d} = [d_1, \cdots, d_n]^T$ and $\boldsymbol{z} = [z_1, \cdots, z_l]^T$, respectively. The random variables are assumed to be independent of each other, and their mean and standard deviation are denoted as $\boldsymbol{\mu} = [\mu_1, \cdots, \mu_l]^T$ and $\boldsymbol{\sigma} = \mathrm{diag}[\sigma_1, \cdots, \sigma_l]^T$, respectively. In many cases, the mean values of the random variables $\boldsymbol{\mu}$ are adopted as the design variables $\boldsymbol{d}$.

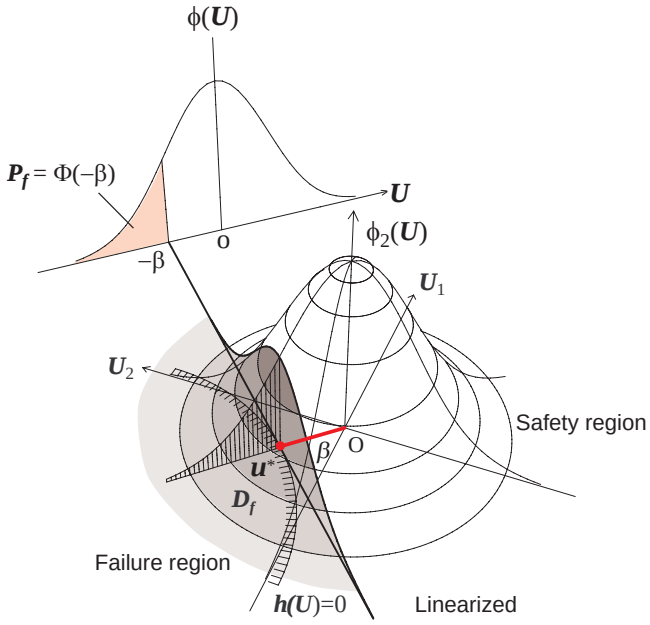

Fig. 1 Concept of FORM. Reliability index β is obtained as the minimum distance from the origin to the limit state surface $h(\boldsymbol{U}) = 0$ in $\boldsymbol{U}$-space, where $\phi_2()$ is a joint density function of the two-dimensional standardized normal distribution. The point that gives the minimum distance is called the the design point $\boldsymbol{u}^*$, where $\beta = \|\boldsymbol{u}^*\|$. The failure probability is approximated as $P_f = \Phi(-\beta)$ by linearizing the limit state function around the design point.

2.1. First-Order Reliability Analysis

The limit state function corresponding to the j-th failure mode is denoted as $g_j(\boldsymbol{d}, \boldsymbol{z})$ $(j = 1, \cdots, k)$, and the failure probability P_{f_j} is defined as the probability that the j-th limit state function takes a negative value:

$$P_{f_j} = P(g_j(\boldsymbol{d}, \boldsymbol{z}) \leq 0). \tag{1}$$

As it is difficult, even impossible, to evaluate this probability, the reliability is evaluated by a Monte Carlo simulation or an approximation method. FORM [Rackwitz and Fiessler, 1978] is one of the main methods for the evaluation of reliability. In FORM, the random vector $\boldsymbol{z}$ is transformed into the standard normal distribution space ($\boldsymbol{U}$-space), and the reliability is evaluated by the reliability index β_j, which is defined as the minimum distance from the origin to the j-th limit state surface in $\boldsymbol{U}$-space (see Fig. 1). The reliability index is obtained through the following problem:

$$\text{Minimize: } \beta_j = \sqrt{\boldsymbol{u}^T \boldsymbol{u}} \tag{2}$$

$$\text{subject to: } h_j(\boldsymbol{d}, \boldsymbol{u}) = 0, \tag{3}$$

where $h_j(\boldsymbol{d}, \boldsymbol{u})$ is the j-th limit state function, formulated in $\boldsymbol{U}$-space, that is transformed from $g_j(\boldsymbol{d}, \boldsymbol{u})$. The limit state function is then linearized around the design point $\boldsymbol{u}^*$. As shown in Fig. 1, the failure probability is approximated by a one-dimensional standardized normal distribution function $\Phi()$:

$$P_{f_j} = \Phi(-\beta_j) \quad (j = 1, \cdots, m). \tag{4}$$

In the RBMO problem, the failure probability constraint (which states that the failure probability should not exceed the upper limit P_j^t, $P_{f_j} \leq P_j^t$) is rewritten using the reliability index as follows:

$$\beta_j = -\Phi^{-1}\left[P(g_j(\boldsymbol{d}, \boldsymbol{z}) < 0)\right] \geq \beta_j^t, \quad (j = 1, \cdots, m) \tag{5}$$

where β_j^t is the target reliability index for the j-th failure mode corresponding to $P_j^t = \Phi(-\beta_j^t)$.

2.2. Formulation of RBMO

In this RBMO problem, the reliability constraints state that the failure probabilities must be lower than the allowable values. This is the only difference from the conventional multiobjective optimization problem. The RBMO problem is formulated as follows:

$$\text{Minimize:} \quad \boldsymbol{F}(\boldsymbol{d}) = (f_1(\boldsymbol{d}), f_2(\boldsymbol{d}), \cdots, f_k(\boldsymbol{d})) \tag{6}$$

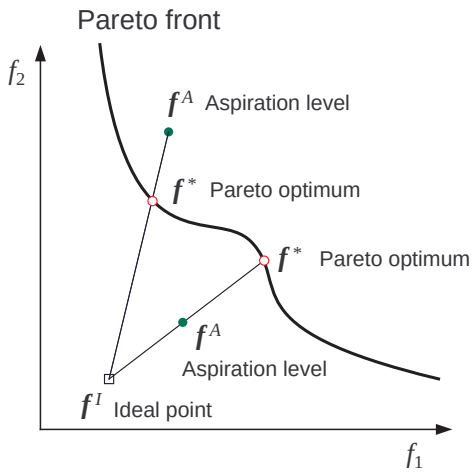

Fig. 2 STOM Pareto solution search process in the objective function space. Pareto solution $\boldsymbol{f}^*$ is obtained as the intersection between the Pareto surface and the line connecting the ideal point $\boldsymbol{f}^I$ and the aspiration point $\boldsymbol{f}^A$.

$$\text{subject to:} \quad \beta_j = -\Phi^{-1}\left[P(g_j(\boldsymbol{d}, \boldsymbol{z}) < 0)\right] \geq \beta_j^t, \qquad (j = 1, \cdots, m) \tag{7}$$

$$\boldsymbol{d}_L \leq \boldsymbol{d} \leq \boldsymbol{d}_U, \tag{8}$$

where $f_i(\boldsymbol{d})$ is the i-th objective function, β_j^t is the allowable value of the reliability index for the j-th failure mode, and $\boldsymbol{d}_U$ and $\boldsymbol{d}_L$ are the upper and lower bounds of the design variables, respectively.

In this study, we adopt a double-loop algorithm using FORM. For further improvement, decoupled methods may be adopted in future.

3. Satisficing Trade-off Method and Automatic Trade-off Analysis

STOM [Nakayama and Sawaragi, 1984] is an interactive multiobjective optimization method that obtains one Pareto solution by solving the min-max problem according to the given aspiration level. STOM can obtain the Pareto solution, even if the Pareto surface is not convex. As shown in Fig. 2, STOM obtains one Pareto solution at the intersection between the Pareto surface and the line connecting the ideal point and the aspiration level. Even if this line does not cross the Pareto surface, STOM will obtain the closest point as a Pareto solution.

3.1. STOM for RBMO

This study applies STOM to RBMO. The flow of STOM with reliability constraints is summarized in Fig. 3, and can be briefly described as follows.

Step 1 The ideal point f_i^I $(i = 1, \cdots, k)$ of each objective is determined. The ideal point is usually determined by solving a single-objective optimization problem considering only the corresponding objective function $f_i(\boldsymbol{d})$. The user then decides the aspiration level f_i^A $(i = 1, \cdots, k)$ for each objective function.

Step 2 The following weighting factor is introduced for each objective function:

$$w_i = \frac{1}{f_i^A - f_i^I}, \qquad (i = 1, \cdots, k). \tag{9}$$

The multiobjective optimization problem is then formulated as follows:

$$\text{Minimize:} \ \max_{i \in [1,k]} w_i(f_i(\boldsymbol{d}) - f_i^I) + \alpha \sum_{i=1}^{k} w_i f_i(\boldsymbol{d}) \tag{10}$$

$$\text{subject to:} \ \beta_j = -\Phi^{-1}\left[P(g_j(\boldsymbol{d}, \boldsymbol{z}) < 0)\right] \geq \beta_j^t \quad (j = 1, \cdots, m) \tag{11}$$

$$\boldsymbol{d}^L \leq \boldsymbol{d} \leq \boldsymbol{d}^U, \tag{12}$$

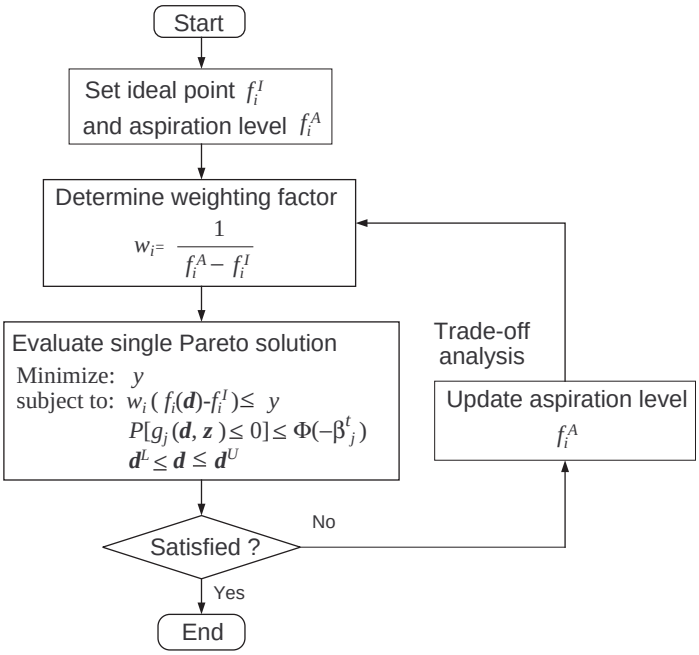

Fig. 3 Flowchart of RBMO using STOM. First, set the ideal point f_i^I and the aspiration level f_i^A. Then, evaluate the weighting factor w_i. The multiobjective optimization problem is formulated as a single-objective optimization based on STOM. The Pareto solution is obtained using a nonlinear mathematical programming method, where the reliability constraints are evaluated using FORM. If the obtained Pareto solution does not satisfy the user, the optimization is repeated after the aspiration level f_i^A has been updated. The automatic trade-off analysis is one method of determining the aspiration level.

where α is a small positive number (e.g., 10^{-6}) used to avoid convergence to weak Pareto solutions.

Step 3 The min-max problem in Eq. (10) is transformed into the following equivalent single-objective function problem. For this purpose, we introduce the auxiliary design variable y.

$$\text{Minimize: } y + \alpha \sum_{i=1}^{k} w_i f_i(\boldsymbol{x}) \tag{13}$$

$$\text{subject to: } \beta_j = -\Phi^{-1}\left[P(g_j(\boldsymbol{d}, \boldsymbol{z}) < 0)\right] \ge \beta_j^t \quad (j = 1, \cdots, m) \tag{14}$$

$$w_i(f_i(\boldsymbol{d}) - f_i^I) - y \le 0 \quad (i = 1, \cdots, k) \tag{15}$$

$$\boldsymbol{d}^L \le \boldsymbol{d} \le \boldsymbol{d}^U, \tag{16}$$

where Eq. (15) denotes the auxiliary constraints converted from the objective functions.

The single solution that lies on the Pareto set is obtained according to the aspiration level, as shown in Fig. 2.

Step 4 If the user is satisfied with the optimum solution obtained from the equivalent problem, terminate the search process. Otherwise, update the aspiration level f_i^A $(i = 1, \cdots, k)$ and return to Step 2.

Under STOM, a nonlinear programming method can be adopted to obtain a single Pareto set. Therefore, it is much more computationally efficient than evolutionary multiobjective optimization methods. In addition, an accurate, uniformly distributed, and diverse Pareto set can be obtained by parametrically changing the aspiration level. Accordingly, STOM is a more efficient algorithm than evolutionary methods.

3.2. Automatic Trade-off Analysis

"Step 4" requires the aspiration level to be updated. Several methods have been proposed for this purpose [Kitayama and Yamazaki, 2012, Nakayama, 1992], and this study adopts the automatic trade-off analysis [Nakayama, 1992].

In updating the aspiration level, the user must identify which objective functions must be improved and which can be relaxed. Appropriate values of the objective functions can then be determined, and these are directly reflected in the

aspiration level. However, users often overestimate the values to be improved and underestimate those to be relaxed. In such cases, it is very difficult to obtain a satisfactory Pareto solution.

The automatic trade-off analysis [Nakayama, 1992] can resolve this problem by automatically determining a reasonable aspiration level based on a sensitivity analysis.

Consider the unconstrained multiobjective optimization problem that ignores the reliability and side constraints of Eq. (13). The Lagrangian is written as:

$$L(\boldsymbol{d}, y, \boldsymbol{\lambda}) = y + \sum_{i=1}^{k}(\lambda_i + \alpha) w_i f_i(\boldsymbol{d}) - \sum_{i=1}^{k} \lambda_i w_i (f_i^I + y), \tag{17}$$

where $\boldsymbol{\lambda} = (\lambda_1, \lambda_2, \cdots, \lambda_k)^T$ contains the Lagrange multipliers of the objective functions. From the stationary condition with respect to the design variables $\boldsymbol{d}$, the following equation is obtained:

$$\sum_{i=1}^{k}(\lambda_i + \alpha) w_i \nabla f_i(\boldsymbol{d}) = \boldsymbol{0}. \tag{18}$$

Under some linearly independent approximations, Eq. (18) can be re-written using a small perturbation $\Delta f_i \approx \nabla f_i$.

Here, the objective functions are classified into two groups: (i) the set of objectives to be improved I_I, and (ii) the set of objectives that will be sacrificed I_R. The updated aspiration level for the set I_I is determined as follows:

$$f_j^A = f_j^* + \Delta f_j, \qquad j \in I_I, \tag{19}$$

where f_j^* is the current objective function value and Δf_j is the desired value for improvement. From Eq. (18), the sum of Δf_j in I_I should be equal to the sum of Δf_j in I_R. When the sacrificed values are evenly distributed across each objective in I_R, this is evaluated from Eq. (18) as follows:

$$\Delta f_j = \frac{-1}{k_I(\lambda_j + \alpha) w_j} \sum_{i \in I_I} w_i(\lambda_i + \alpha)\Delta f_i \qquad j \in I_R, \tag{20}$$

where k_I is the number of objectives in set I_I. That is, the aspiration value in I_R is determined from Eq. (20) as:

$$f_j^A = f_j^* + \Delta f_j, \qquad j \in I_R. \tag{21}$$

Since this determination is based on a linear approximation of the Pareto surface, the process should be repeated several times for the nonlinear problem to obtain a satisfactory Pareto solution.

4. Numerical Examples

Two numerical examples are given to demonstrate the efficiency of the proposed method.

The first is a mathematical example with a non-convex Pareto set. We demonstrate that the proposed method obtains a more accurate, uniformly distributed, and diverse Pareto set by parametrically changing the aspiration level, despite the Pareto surface being non-convex. Then, the tracking ability of Pareto solutions with the same aspiration level is investigated in terms of the target reliability. We clarify that the shift in the dominant failure mode influences the kink in the tracking trajectory in terms of the target reliability.

The second is an engineering design example that considers the problem of automobile crashworthiness. We show that, compared with the hybrid-type MOPSO [Kogiso et al., 2012, Kogiso and Kawaji, 2013], STOM can obtain a more accurate and uniformly distributed Pareto set by parametrically changing the aspiration level. We then demonstrate that the automatic trade-off analysis gives the desired Pareto solution by updating the aspiration level, even when the Pareto surface is nonlinear.

4.1. Example 1: Mathematical Example

Consider the following problem that has both a convex and non-convex feasible region [Liang et al., 2004] (see Fig. 4):

$$g_1(\boldsymbol{d}) = \frac{d_1^2 d_2}{20} - 1 \geq 0 \tag{22}$$

$$g_2(\boldsymbol{d}) = \frac{(d_1 + d_2 - 5)^2}{30} + \frac{(d_1 - d_2 - 12)^2}{120} - 1 \geq 0 \tag{23}$$

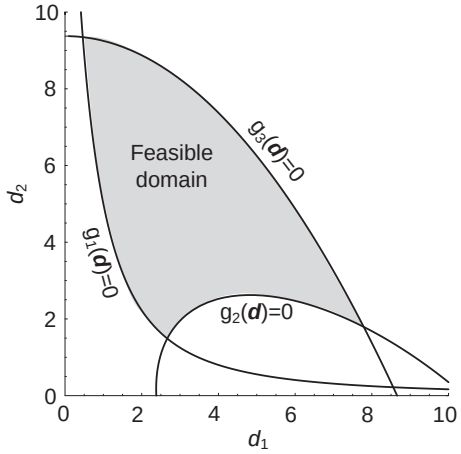

Fig. 4 Feasible domain of Example 1.

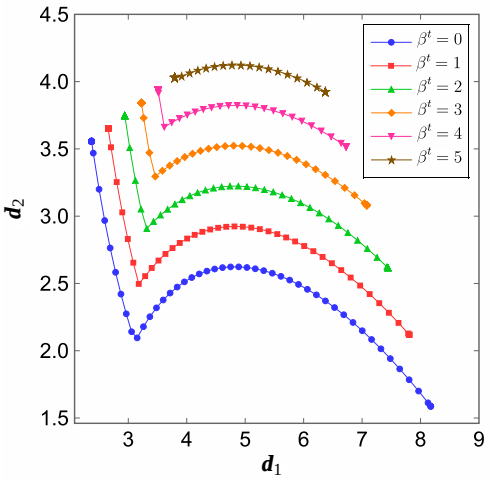

Fig. 5 Pareto set of Example 1 in the design variable space. Each Pareto solution is obtained by parametrically changing the aspiration level. The deterministic Pareto set corresponding to $\beta^t = 0$ lies on the constraint boundary, either $g_1 = 0$ or $g_2 = 0$. As the target reliability value β^t becomes larger, the Pareto set shifts up and right, inside the feasible region.

$$g_3(\boldsymbol{d}) = \frac{80}{d_1^2 + 2d_2 + 5} - 1 \geq 0$$
$$0 \leq d_i \leq 10, \qquad (i = 1, 2). \tag{24}$$

The design variables $d_i, (i = 1, 2)$ are defined as the mean values of the random variables $\boldsymbol{x}$. These are assumed to have independent normal distributions, $N(d_i, \sigma_i^2), (i = 1, 2)$, where σ_i is set to 3.0 in this study.

Consider the following two objective function problems:

$$f_1(\boldsymbol{d}) = 3d_1 + d_2 \tag{25}$$
$$f_2(\boldsymbol{d}) = -d_1 + d_2 + 10.$$

The minimum points of f_1 and f_2 are (0,0) and (0,10), respectively. The Pareto set under the deterministic condition lies on the boundary of the feasible region, close to the d_1-axis in the design variable space, that is, the lower direction in Fig. 4. The Pareto sets obtained under several target reliability index values β_t are illustrated in Fig. 5, where the Pareto curves are obtained by parametrically changing the aspiration level. It is found that the Pareto set moves toward the upper right of Fig. 4 as the target reliability index becomes larger.

STOM can track the shift in Pareto solutions with the same aspiration level in terms of the target reliability. This tracking ability is a major difference between STOM and evolutionary methods, which cannot track the shift of each Pareto solution, though the change in the whole Pareto set can be tracked. Figure 6 shows the shift of some Pareto solutions in

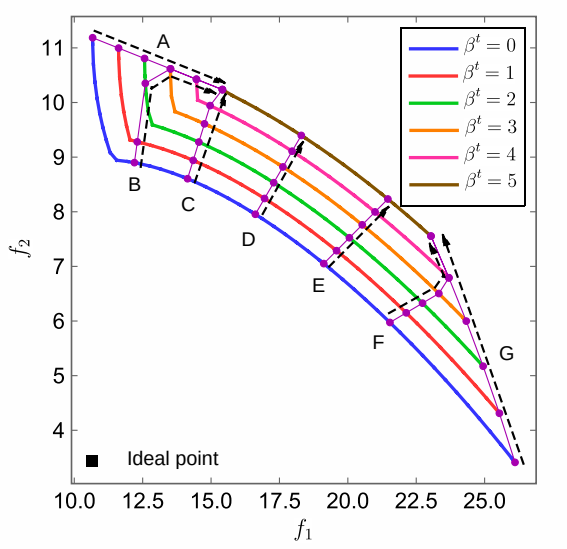

Fig. 6 Flows A to G correspond to the parametric shift in Pareto solutions with the same aspiration level in terms of the target reliability index in Example 1. The kinks correspond to shifts in the active constraints, as shown in Table 1.

the objective function space. The curves indicate the Pareto set, and arrows labeled A–G indicate the shift in the Pareto solution with the same aspiration level.

The Pareto solutions around the center of the Pareto curves shift radially from the ideal point as the target reliability value increases. Pareto solutions close to the edge of the Pareto curves are kinked. For example, the flow B around the upper-left position in Fig. 6 merges with flow A, which is the upper-left edge of the Pareto curve. Similarly, flow F merges with flow G.

The kinks correspond to a shift in mode. Table 1 shows the mode shifts for three typical flows, where f_1 and f_2 are the objective function values. A value of 0 in g_j indicates that the constraint is active, where g_1, g_2, and g_3 correspond to the reliability constraints and g_4 and g_5 are constraints on the auxiliary objective functions. When both g_4 and g_5 are active, the given Pareto solution lies on the line connecting the aspiration level and the ideal points. Otherwise, the Pareto solution does not follow the aspiration level. Additionally, the active reliability constraints are changed.

4.2. Example 2: Car Side-Impact Problem

As an engineering design example, the RBMO of the automobile crashworthiness problem [Sinha,2007] is evaluated by the proposed STOM. This problem is used as one of the RBMO benchmarks, and consists of two objective functions in terms of nine design variables under nine reliability constraints, where the design variables are set as the mean values of the random variables. The problem formulation is summarized in Table 2, where the reliability constraints are formulated as follows:

$$P_f(g_j \geq 0) \leq \Phi(-\beta_j^t), (j = 1, \cdots, 9). \tag{26}$$

Figure 7 compares the Pareto set obtained by the proposed method, in which we can parametrically change the aspiration level, and that given by the hybrid-type MOPSO [Kogiso et al., 2012]. It can be seen that STOM obtains more accurate and uniformly distributed Pareto sets than MOPSO. In particular, as it is a stochastic approach, MOPSO found it difficult to obtain the upper-left region with the smaller value of f_1. However, STOM obtains the Pareto solution according to the aspiration level. In addition, the arrows in Fig. 7 (b) indicate the shift in Pareto solution with the same aspiration level in terms of the target reliability values.

4.3. Automatic Trade-Off Analysis in Example 2

The examples above illustrate the accuracy of the Pareto solutions obtained under STOM by parametrically changing the aspiration level.

This subsection demonstrates how the automatic trade-off analysis works for the car side-impact problem. Assume that the desired structural weight (f_1) is 19.0 kg under the target reliability $\beta_t = 3.0$. The first aspiration level is set

Table 1 Tracking of Pareto solutions in terms of target reliability β^t in Example 1. Symbols of flows B, C, and F correspond to those in Fig. 6. f_1 and f_2 are the objective function values. "0" in g_j, $(j = 1, \cdots, 5)$ denotes that the constraint is active. g_1–g_3 correspond to the reliability constraints, and g_4, g_5 are constraints on the auxiliary objective functions.

(a) Flow B

	Objectives		Reliability const.			Auxiliary const.	
β^t	f_1	f_2	g_1	g_2	g_3	g_4	g_5
0	12.20	8.90		0		0	0
1	12.30	9.28		0		0	0
2	12.60	10.35	0			0	0
3	13.52	10.62	0			0	
4	14.47	10.43	0			0	
5	15.41	10.24	0			0	

(b) Flow C

	Objectives		Reliability const.			Auxiliary const.	
β^t	f_1	f_2	g_1	g_2	g_3	g_4	g_5
0	14.14	8.60		0		0	0
1	14.35	8.94		0		0	0
2	14.55	9.28		0		0	0
3	14.76	9.61		0		0	0
4	14.97	9.94		0		0	0
5	15.41	10.24	0			0	

(c) Flow F

	Objectives		Reliability const.			Auxiliary const.	
β^t	f_1	f_2	g_1	g_2	g_3	g_4	g_5
0	21.54	5.97		0		0	0
1	22.13	6.15		0		0	0
2	22.73	6.33		0		0	0
3	23.33	6.50		0		0	0
4	23.69	6.79		0	0	0	0
5	23.04	7.55		0	0		0

to $\boldsymbol{f}^{A1} = (19.0, 14.0)$, where the desired value of the door velocity f_2 is determined arbitrarily. The evolution of this automatic trade-off approach prior to obtaining the desired solution with $f_1 = 19.0$ can be described as follows:

1st trial Starting from the first aspiration level $\boldsymbol{f}_1^A = (19.0, 14.0)$, the obtained Pareto solution is $\boldsymbol{f}^{(1)} = (20.254, 14.197)$. The value of f_1 is larger than the desired value.

2nd trial To obtain the desired structural weight of 19.0 kg, Δf_1 is set to $20.254 - 19.0 = 1.254$, and the relaxed value of the door velocity is obtained as 14.324 from Eq. (20). That is, the aspiration level is set to $\boldsymbol{f}_2^A = (19.0, 14.342)$. The obtained Pareto solution is $\boldsymbol{f}^{(2)} = (19.487, 14.446)$. The value of f_1 is closer to the desired value, but is still too large.

3rd trial Set $\Delta f_1 = 19.487 - 19.0 = 0.487$, and update the aspiration level to $\boldsymbol{f}_3^A = (19.0, 14.792)$ according to Eq. (20). The obtained Pareto optimal solution is $\boldsymbol{f}^{(3)} = (19.0, 14.792)$. The desired solution has been successfully obtained, and the trade-off analysis is complete.

The evolution of the automatic trade-off process is summarized in Fig. 8 and Table 3. We can see from Fig. 8 that the second and subsequent aspiration levels correspond to the linear approximation of the Pareto curve in the objective function space.

5. Conclusion

This study has proposed a new RBMO method using STOM. Through numerical examples, the following advantages over the hybrid-type MOPSO were demonstrated:

- Accurate, uniformly distributed, and diverse Pareto sets are obtained by parametrically changing the aspiration level. Since each Pareto solution is obtained through a mathematical programming method, STOM obtains more accurate Pareto sets than those given by the hybrid-type MOPSO.
- The proposed method makes it possible to track not only the change in the whole Pareto surface, but also the changes in each Pareto solution. We demonstrated the ability to track Pareto solutions with the same aspiration level in

Table 2 Formulation of RBMO for a car side-impact problem [Sinha,2007]. This problem has two objective functions under nine reliability constraints for nine design variables that correspond to the mean values of the random variables. The objective and constraint functions are evaluated by polynomial approximation.

(a) Nine design variables, side constraints, and covariance in random variables

Name	Variable	Lower bound	Upper bound	Cov. ($=\sigma/\mu$)
Thickness of B-pillar inner (mm)	d_1	0.5	1.5	0.03
Thickness of B-pillar reinforcement (mm)	d_2	0.5	1.5	0.03
Thickness of floor side inner (mm)	d_3	0.5	1.5	0.03
Thickness of cross members (mm)	d_4	0.5	1.5	0.03
Thickness of door beam (mm)	d_5	0.5	1.5	0.03
Thickness of door belt line reinforcement (mm)	d_6	0.5	1.5	0.03
Thickness of roof rail (mm)	d_7	0.5	1.5	0.03
Material yield stress for B-pillar inner (GPa)	d_8	0.192	0.750	0.02
Material yield stress for floor side inner (GPa)	d_9	0.192	0.750	0.02

(b) Two objective functions

Weight	$f_1 = 1.98 + 4.9d_1 + 6.67d_2 + 6.98d_3 + 4.01d_4 + 1.78d_5 + 2.73d_7$
Door velocity	$f_2 = 16.45 - 0.489d_3d_7 - 0.843d_5d_6$

(c) Nine constraints

Abdomen load	$g_1 = 1.163 - 0.3717d_2d_4 - 0.484d_3d_9$
Rib deflection upper	$g_2 = 28.98 + 3.818d_3 - 4.2d_1d_2 + 6.63d_6d_9 - 7.70d_7d_8$
Rib deflection middle	$g_3 = 33.86 + 2.95d_3 - 5.057d_1d_2 - 11.0d_2d_8 - 9.98d_7d_8 + 22.0d_8d_9$
Rib deflection lower	$g_4 = 46.36 - 9.9d_2 - 12.9d_1d_8$
Pubic symphysis force	$g_5 = 4.72 - 0.5d_4 - 0.19d_2d_3$
B-Pillar velocity	$g_6 = 10.58 - 0.674d_1d_2 - 1.95d_2d_8$
VC upper	$g_7 = 0.261 - 0.0159d_1d_2 - 0.188d_1d_8 - 0.019d_2d_7 + 0.0144d_3d_5 + 0.08045d_6d_9$
VC middle	$g_8 = 0.214 + 0.00817d_5 - 0.131d_1d_8 - 0.0704d_1d_9 + 0.031d_2d_6 - 0.018d_2d_7 + 0.021d_3d_8 + 0.121d_3d_9 - 0.00364d_5d_6$
VC lower	$g_9 = 0.74 - 0.61d_2 - 0.163d_3d_8 - 0.18d_7d_9 + 0.227d_2^2$

terms of the target reliability, and showed that the tracking path is sometimes kinked because of changes in the dominant failure mode.

- The automatic trade-off analysis is effective even for nonlinear Pareto surfaces.

In future work, a decoupled reliability-based design optimization method will be adopted to establish a computationally efficient technique.

Acknowledgment

This research is partially supported by JSPS KAKENHI 26249131.

References

Chen, X., Hasselman, T. K., and Neill, D. J., Reliability based structural design optimization for practical applications, Proceedings of 38th AIAA/ASME/ASCE/AHS/ASC Structures, Structural Dynamics and Materials Conference, Vol. 4, (1997), AIAA-97-1403, pp. 2724-2732.

Choi, S-K., Grandhi, R. V., and Canfield, R. A., Reliability-based structural design, (2007), Springer-Verlag.

Deb, K., Pratap, A., Agarwal S., and Meyarivan T., A fast and elitist multiobjective genetic algorithm: NSGA-II, IEEE Transactions on Evolutionary Computation, Vol. 6, No. 2 (2002), pp. 182-197.

Deb, K., Padmanabhan, D., Gupta, S., and Mall, A. K., Reliability-based optimization using evolutionary algorithms, IEEE Transactions on Evolutionary Computation, Vol. 13, No. 5, (2009), pp. 1054-1074.

Du, X. and Chen, W., Sequential optimization and reliability assessment method for efficient probabilistic design, ASME Journal of Mechanical Design, Vol. 126, No. 2 (2004), pp. 225-233.

Greiner, J. and Hajela, P., Truss topology optimization for mass and reliability considerations – co-evolutionary multiobjective formulations. Structural and Multidisciplinary Optimization, Vol. 45, No. 4 (2012), pp. 589-613.

Kitayama, S. and Yamazaki, K., Compromise point incorporating trade-off ratio in multi-objective optimization, Applied Soft Computing, Vol. 12, No. 8 (2012), pp. 1959-1964.

Kogiso, N., Kawaji, S., Ohara, M., Ishigame, A., and Sato, K., Reliability-based multiobjective optimization using hybrid-

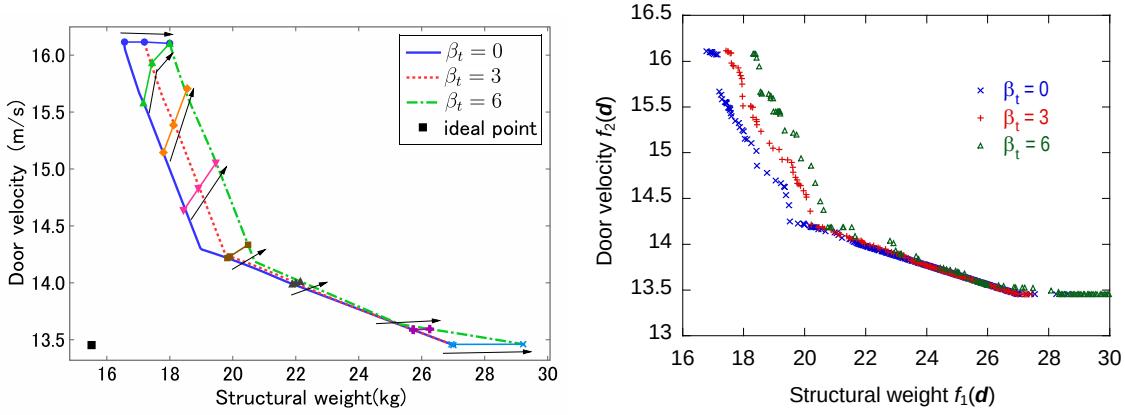

(a) STOM (b) Hybrid-type MOPSO [Kogiso et al., 2012]

Fig. 7 Comparison of Pareto sets in the car side-impact problem [Sinha,2007]. STOM obtains more accurate and uniformly distributed Pareto solutions than those given by the hybrid-type MOPSO.

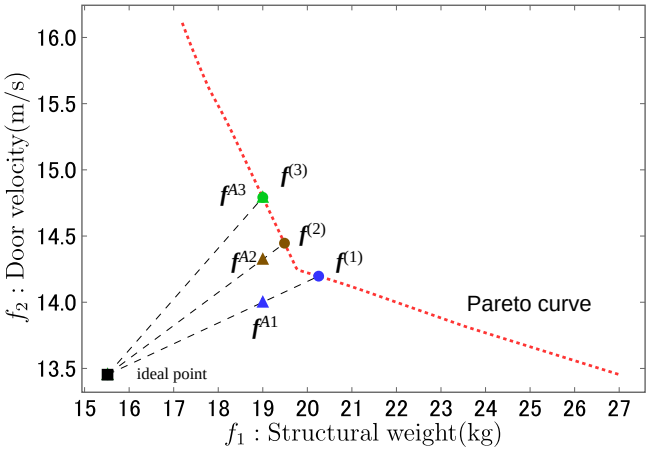

Fig. 8 History of the search for a Pareto solution with $f_1 = 19.0$ using automatic trade-off analysis. Set the aspiration level $\boldsymbol{f}^{A1}$ with $f_1 = 19.0$ and obtain the Pareto solution $\boldsymbol{f}^{(1)}$. As the value of f_1 at $\boldsymbol{f}^{(1)}$ is larger than the desired value, the aspiration level is updated to $\boldsymbol{f}^{A2}$, and the Pareto solution $\boldsymbol{f}_{(2)}$ is obtained. As the value of f_1 is still too large, the aspiration level is updated again to $\boldsymbol{f}^{A3}$. Finally, the desired value is obtained as $\boldsymbol{f}^{(3)}$. The detailed values are listed in Table 3.

type multiobjective PSO algorithms incorporating sensitivity analysis on constraints, Transactions of the Japan Society of Mechanical Engineers, Series C, Vol. 78, No. 790 (2012), pp. 2229-2240 (in Japanese).

Kogiso, N. and Kawaji, S., Convergence improvement of reliability-based multiobjective optimization using hybrid MOPSO, Proceedings of 10th World Congress on Structural and Multidisciplinary Optimization, No. 5276, (2013), pp. 1-10.

Li, F., Luo, Z., and Sun, G., Reliability-based multiobjective design optimization under interval uncertainty, Computer Modeling in Engineering Science, Vol. 74, No. 1 (2011), pp. 39-64.

Liang, J, Mourelatos, Z. P., and Tu, J., A Single-loop method for reliability-based design optimization, Proceedings of ASME 2004 International Design Engineering Technical Conferences and Computers and Information in Engineering Conference, No. DETC2004-57255, (2004), pp. 1-12.

Madsen, H. O., Krenk, S., and Lind, H., Methods of structural safety, (1986), Prentice-Hall.

Mittinen, K M., Nonlinear multiobjective optimization, (2004), Kluwer Academic Publishers.

Nakayama, H. and Sawaragi, Y., Satisficing trade-off method for multiobjective programming, Lecture Notes in Economics and Mathematical Systems, Vol. 229 (1984), pp. 113-122.

Nakayama, H., Trade-off analysis using parametric optimization techniques, European Journal of Operational Research, Vol. 60, No. 1 (1992), pp. 87-98.

Nakayama, H., Kaneshige, K., Takemoto, S., and Watada, Y., An application of a multiobjective programming technique to construction accuracy control of cablestayed bridges, European Journal of Operational Research, Vol. 83, No. 3 (1995), pp. 731-738.

Table 3 Iteration history of the search for a Pareto solution with $f_1 = 19.0$ using automatic trade-off analysis. See Fig. 8.

Iteration	Aspiration level		Pareto solution	
	f_1	f_2	f_1	f_2
1	19.0	14.0	20.254	14.197
2	19.0	14.342	19.487	14.446
3	19.0	14.792	19.0	14.792

Rackwitz, R. and Fiessler, B., Structural reliability under combined random load sequences, Computer and Structures, Vol. 9, No. 5 (1978), pp. 489-494.

Rangavajhala, S. and Mahadevan, S., Joint probability formulation for multiobjective optimization under uncertainty, Journal of Mechanical Design, Vol. 133, No. 5 (2011), p. 051007.

Reyes-Sierra, M. and Coello Coello, C. A., Multi-objective particle swarm optimizers: a survey of the state-of-the-art, International Journal of Computational Intelligence Research, Vol. 2, No. 3 (2006), pp. 287-308.

Sinha, K., Reliability-based multiobjective optimization for automotive crashworthiness and occupant safety, Structural and Multidisciplinary Optimization, Vol. 33, No. 3, (2007), pp. 255-268.

Valdebenito, M. A. and Schuëller, G. I., A survey on approaches for reliability-based optimization, Structural and Multidisciplinary Optimization, Vol. 42, No. 5 (2010), pp. 645-663.